

Study of factors limiting electron mobility in InSb quantum wells

S. J. Chung,^{a)} K. J. Goldammer, S. C. Lindstrom, M. B. Johnson, and M. B. Santos
*Department of Physics and Astronomy and Laboratory for Electronic Properties of Materials,
University of Oklahoma, Norman, Oklahoma 73019*

(Received 5 October 1998; accepted 27 November 1998)

We observe a significant increase in InSb quantum-well mobility when remote doping of $\text{Al}_{0.09}\text{In}_{0.91}\text{Sb}$ barriers is accomplished by three layers, rather than one layer, of Si δ doping. At 7 K, the electron mobility in single quantum-well structures grown on GaAs substrates is as high as $280\,000\text{ cm}^2/\text{V s}$ with an electron density of $2.33 \times 10^{11}\text{ cm}^{-2}$. The density of oriented abrupt steps and square-mound features on the sample surface correlates with the electron mobility in the well.

© 1999 American Vacuum Society. [S0734-211X(99)04203-1]

I. INTRODUCTION

The small band gap of InSb results in the highest intrinsic electron mobility, smallest effective mass, and largest electron g factor among all binary III–V semiconductors. These unique characteristics make electron systems in InSb attractive, not only for low-temperature transport studies,^{1,2} but also for device applications such as high-speed transistors³ and sensitive magnetoresistors.⁴ However, the lack of ideal substrate and barrier materials for InSb makes fabrication of a high-quality two-dimensional electron gas (2DEG) challenging.

Recently, we reported high-mobility 2DEGs in remotely doped InSb quantum wells with $\text{Al}_{0.09}\text{In}_{0.91}\text{Sb}$ barriers on GaAs substrates. The lattice mismatch between the well and barrier layers is $\approx 0.5\%$. Our multiple quantum-well structures, with thick buffer layers to accommodate the large lattice mismatch ($\sim 14\%$) between the substrate and epilayers, have the highest room-temperature mobility ($\sim 41\,000\text{ cm}^2/\text{V s}$) ever reported for semiconductor quantum wells. However, this value is still significantly lower than the $\sim 60\,000\text{ cm}^2/\text{V s}$ that others^{5–7} and we observe in undoped InSb layers on GaAs substrates. In this article, we focus on two scattering sources that limit the mobility in our quantum-well structures: remote ionized donors and dislocations. Characterization of these factors is an important step toward reaching the intrinsic mobility of InSb in quantum-well structures.

II. EXPERIMENT

The layer sequence for all $\text{Al}_x\text{In}_{1-x}\text{Sb}/\text{InSb}$ quantum-well structures in this study is shown in Fig. 1. All growths were performed in an Intevac Gen II molecular beam epitaxy system using procedures similar to those reported previously.⁸ A $1\text{ }\mu\text{m}$ AlSb nucleation layer, which has a lattice constant about midway between GaAs and $\text{Al}_{0.09}\text{In}_{0.91}\text{Sb}$, was grown on a semi-insulating GaAs (001) substrate. The buffer layers that follow are $\sim 1\text{ }\mu\text{m}$ of $\text{Al}_{0.09}\text{In}_{0.91}\text{Sb}$, a ten-period $25\text{ }\text{\AA}$ $\text{Al}_{0.09}\text{In}_{0.91}\text{Sb}/25\text{ }\text{\AA}$ InSb strained layer superlattice, and $2\text{ }\mu\text{m}$ of $\text{Al}_{0.09}\text{In}_{0.91}\text{Sb}$. The substrate temperature of $T_{\text{tr}} + 50 \pm 5\text{ }^\circ\text{C}$ during buffer layer growth was lowered to $T_{\text{tr}} - 20$

$\pm 5\text{ }^\circ\text{C}$ prior to the deposition of the first Si δ -doped layer in order to minimize Si dopant compensation.⁹ Substrate temperatures were calibrated through changes in the static (Sb flux only) reflection high-energy electron diffraction pattern upon crossing the transition temperature, $T_{\text{tr}} \sim 390\text{ }^\circ\text{C}$, at which the $\text{Al}_{0.09}\text{In}_{0.91}\text{Sb}$ surface reconstruction changes between $c(4 \times 4)$ and pseudo- (1×3) .

A Si δ -doped layer, with a net donor density N_1 , is placed in each of the two adjacent $\text{Al}_{0.09}\text{In}_{0.91}\text{Sb}$ barrier layers. These two δ -doped layers are located a distance d (the spacer thickness) from the InSb well and supply electrons to the $300\text{-}\text{\AA}$ -thick well. A $1000\text{-}\text{\AA}$ -thick $\text{Al}_{0.09}\text{In}_{0.91}\text{Sb}$ layer is grown to place the third Si δ -doped layer far from the well in order to minimize ionized dopant scattering. The third Si δ -doped layer is located near the surface to provide $N_2 \sim 2 \times 10^{12}\text{ cm}^{-2}$ electrons for surface states.

Hall effect measurements at magnetic fields up to 0.25 T and temperatures between 7 and 300 K were performed on $5 \times 5\text{ mm}$ samples using a closed-cycle He refrigerator with a resistive heater. Electrical contact was made at each corner of the sample by alloying In at $\sim 230\text{ }^\circ\text{C}$ in a $\text{H}_2(20\%)/\text{N}_2(80\%)$ atmosphere for 5 min . Ohmic contact was verified through observation of linear current–voltage characteristics.

The atomic force microscopy study was performed in air using a Topometrix atomic force microscope in noncontact phase mode. The high-resonant-frequency silicon tip had an aspect ratio of approximately 3:1 and a radius of curvature less than $200\text{ }\text{\AA}$.

III. RESULTS AND DISCUSSION

Two series of $\text{InSb}/\text{Al}_{0.09}\text{In}_{0.91}\text{Sb}$ quantum-well structures were grown to see how electrical properties are affected by the proximity and density of ionized donors. The first series consists of seven samples with the same nominal structure except for the spacer thickness which is varied from $d = 200$ to $1000\text{ }\text{\AA}$. The net donor density of the two δ -doped layers near the well is $N_1 \sim 2 \times 10^{11}\text{ cm}^{-2}$. The second series consists of five samples that repeat structures from the first series except for a higher doping density in the two δ -doped layers near the well ($N_1 \sim 3.6 \times 10^{11}\text{ cm}^{-2}$). The densities

^{a)}Corresponding author; electronic mail: chung@mail.nhn.ou.edu

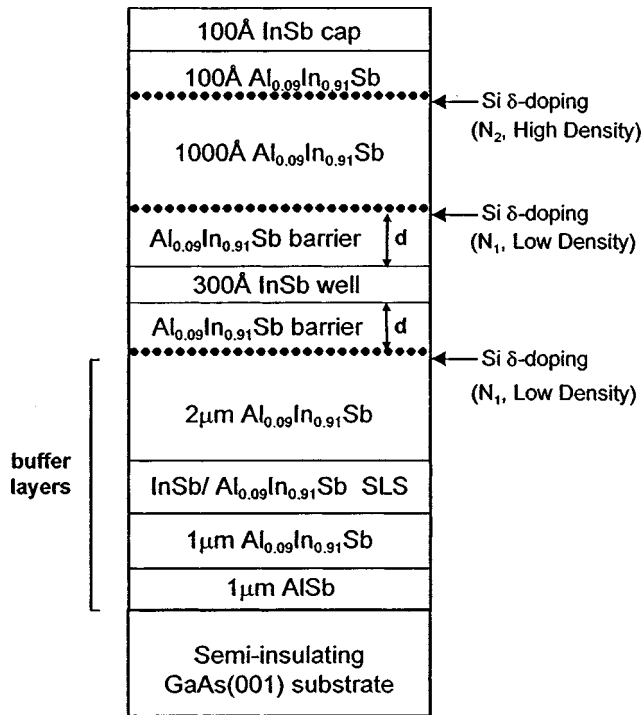


FIG. 1. Layer sequence for a single quantum-well structure.

and mobilities of electrons in the well at 7 K are shown in Fig. 2. Open circles represent the first series and filled circles represent the second series.

As shown in Fig. 2(a), the electron density in the first series increases from $1.84 \times 10^{11} \text{ cm}^{-2}$ to $3.45 \times 10^{11} \text{ cm}^{-2}$ as the spacer thickness is decreased from 1000 to 200 Å. To explain this dependence, a simple electrostatic model was used to calculate the expected electron density as a function of spacer thickness. The results of the calculation are shown as a solid line in Fig. 2(a). In this model, the Fermi energy in the doped layers is assumed fixed at the conduction band edge. Strain and the nonparabolic dispersion relation in the well are taken into account but the effects of band bending are ignored. The assumed InSb/ $\text{Al}_{0.09}\text{In}_{0.91}\text{Sb}$ conduction band offset is 60% of the band gap difference, an approximate value that agrees with optical measurements in InSb/ $\text{Al}_{0.09}\text{In}_{0.91}\text{Sb}$ structures.¹⁰ For comparison, results are also shown (dashed line) for a calculation using a conduction band offset of 55%.

The measured densities in the first series of samples (open circles) are increasingly overestimated by the calculation as d is decreased. Such behavior may result from a donor density that is not high enough to pin the Fermi level in the δ -doped layer. In support of this interpretation, the second series of samples shows better agreement with the calculated values, although a discrepancy still exists between the observed and predicted data. This discrepancy may be reduced by a calculation that takes band bending into account and uses a more realistic value for the Fermi energy in the δ -doped layer.

Scattering by ionized background impurities, remote ionized donors, rough interfaces, and dislocations are all known to affect the mobility of electrons in remotely doped quan-

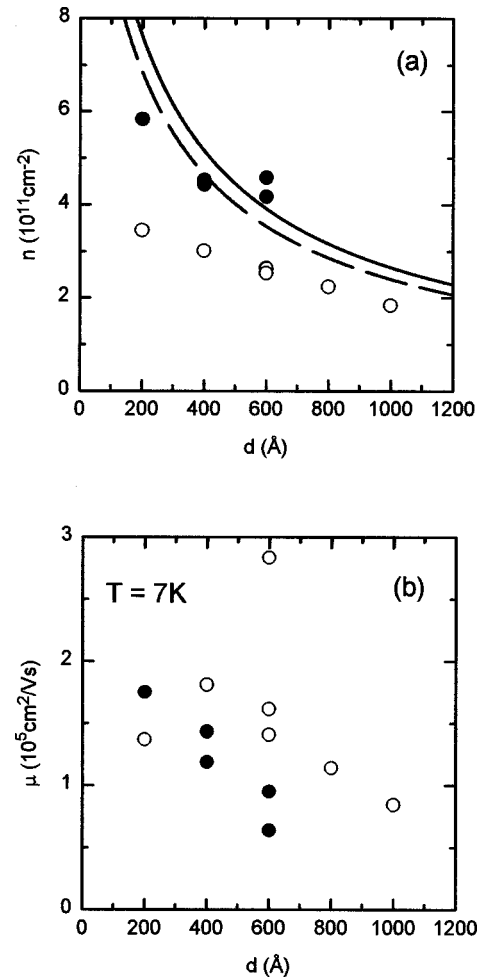


FIG. 2. Electron (a) density and (b) mobility in single quantum-well structures at 7 K. The solid and dashed lines show the predictions of a simple electrostatic model with conduction band offset values of 60% and 55%, respectively.

tum wells. Screening of scattering potentials and the population of a second subband can also be important at high electron densities. As shown in Fig. 2(b), the mobilities for samples in both series depend on d . Although the many factors that affect mobility make it difficult to draw strong conclusions, the data do follow a general trend that implies that remote dopant scattering is important. Nearly every sample in the first series (lower donor density) has a higher mobility than the corresponding sample with the same d in the second series (higher donor density). Moreover, the low-temperature mobilities for every sample in both series are higher than corresponding samples (not shown) with the same d in quantum-well structures with only a single high-density ($\sim 2N_1 + N_2$) δ -doped layer.⁸ The superiority of the samples with three δ -doped layers can be attributed to the additional separation of the largest ionized donor scattering source, N_2 , from the well. A similar enhancement in mobility has been observed in GaAs/ $\text{Al}_x\text{Ga}_{1-x}\text{As}$ heterostructures with multiple δ -doped layers.^{11,12}

The data in Fig. 2(b) show a variation in mobility even for samples with the same nominal structure and doping. This

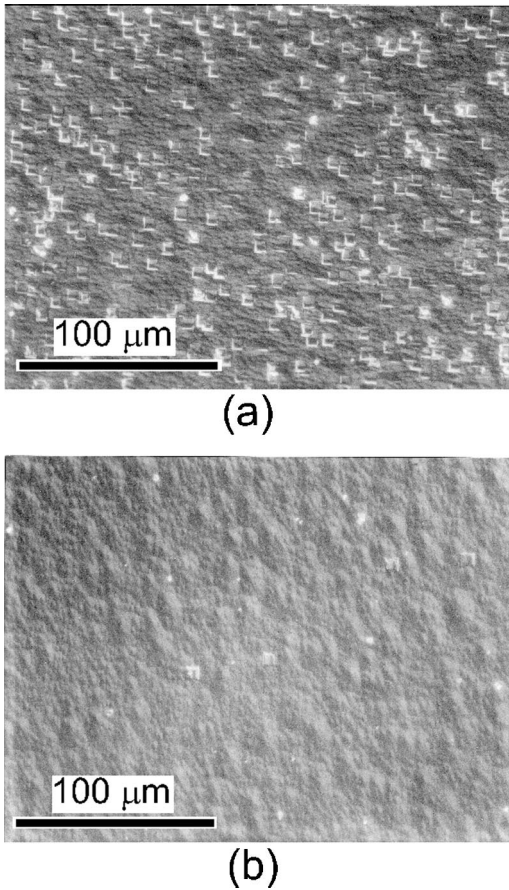


FIG. 3. Nomarski micrographs of surfaces of single quantum-well samples with electron mobilities of (a) 64 000 and (b) 280 000 $\text{cm}^2/\text{V s}$ at 7 K.

spread in mobility values suggests that there are one or more additional factors limiting electron mobility. To gain insight into additional mobility-limiting mechanisms, we characterized the sample surfaces using Nomarski optical microscopy and atomic force microscopy. Figures 3(a) and 3(b) show Nomarski images of two samples (both with $d=600 \text{ \AA}$) whose electron mobilities are 64 000 and 280 000 $\text{cm}^2/\text{V s}$, respectively. In addition to an undulated surface morphology, there are square-mound features defined on all four sides by abrupt steps oriented in the $[110]$ and $[\bar{1}10]$ directions. The noncontact atomic force microscope image in Fig. 4 shows the square-mound features along with oriented abrupt steps and pyramidal features.⁸ The heights of most of the square-mound features vary from ~ 50 to $\sim 500 \text{ \AA}$, while the typical edge length is $\sim 5 \text{ \mu m}$.

The defect density was measured for seven samples (the five with $d=600 \text{ \AA}$ shown in Fig. 2 plus two additional lower-mobility pieces¹³) with mobilities varying from 280 000 to 24 000 $\text{cm}^2/\text{V s}$. The electron mobility as a function of abrupt-step density is shown in Fig. 5. Since each square-mound feature consists of four abrupt steps, all square-mound features were counted as four abrupt steps. Figure 5 indicates a correlation between the density of the abrupt steps and the electron mobility in the well. Since the height of a square-mound feature is comparable to the width of the InSb well, a high density of these surface features will

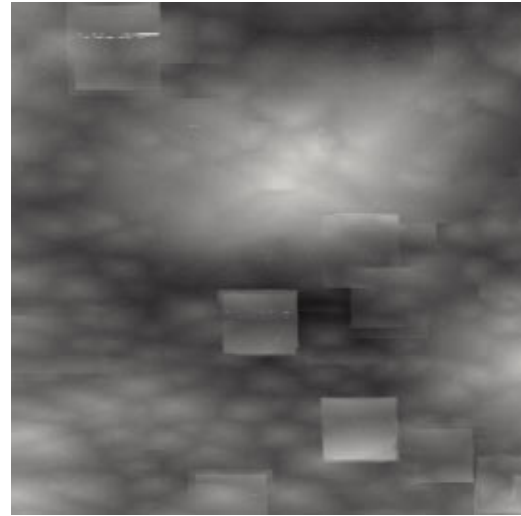


FIG. 4. Noncontact atomic force micrograph of the surface of a single quantum-well sample. The image is a 50 \mu m square region with the gray scale representing a height variation of 1200 \AA .

result in a low mobility as similarly abrupt steps are expected to exist at the InSb/ $\text{Al}_x\text{In}_{1-x}\text{Sb}$ interfaces. The dependence of the defect density on growth parameters and buffer layer composition is currently under investigation.

IV. CONCLUSIONS

In single quantum-well structures, we observe a significant improvement in the low-temperature mobility when the donors required for surface states are separated from those that provide electrons to the quantum well. The mobility also depends on the distance between the well and the δ -doped layers in adjacent barriers. Correlation of surface defects with electron mobility implies that improvements in crystalline quality will lead to higher mobility.

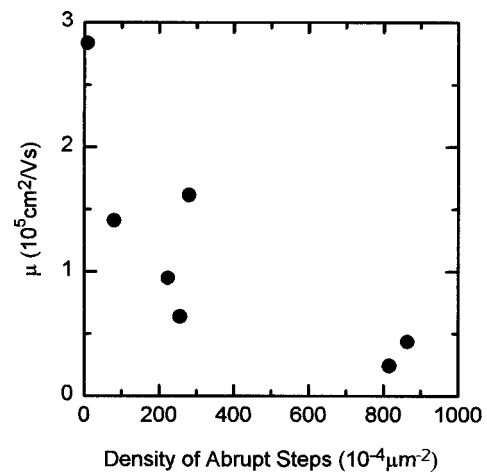


FIG. 5. Electron mobility at 7 K as a function of abrupt-step density.

ACKNOWLEDGMENTS

The authors thank Giti Khodaparast, Robert Meyer, and Niti Goel for technical assistance and useful discussions. This work is supported by NSF Grants No. DMR-9624699 and ECS-9733966.

- ¹T. D. Golding, S. K. Greene, M. Pepper, J. H. Dinan, A. G. Cullis, G. M. Williams, and C. R. Whitehouse, *Semicond. Sci. Technol.* **5**, 311 (1990).
²K. J. Goldammer, S. J. Chung, W. K. Liu, M. B. Santos, J. L. Hicks, S. Raymond, and S. Q. Murphy, *J. Cryst. Growth* (to be published).
³T. Ashley, A. B. Dean, C. T. Elliot, G. J. Pryce, A. D. Johnson, and H. Willis, *Appl. Phys. Lett.* **66**, 481 (1995).
⁴J. Heremans, D. L. Partin, C. M. Thrush, and L. Green, *Semicond. Sci. Technol.* **8**, S424 (1993).
⁵P. E. Thompson, J. L. Davis, J. Waterman, R. J. Wagner, D. Gammon, D. K. Gaskill, and R. Stahlbush, *J. Appl. Phys.* **69**, 7166 (1991).

- ⁶J. R. Soderstrom, M. M. Cumming, J.-Y. Yao, and T. G. Anderson, *Semicond. Sci. Technol.* **7**, 337 (1992).
⁷G. Singh, E. Michel, C. Jelen, S. Silvken, J. Xu, P. Bove, I. Ferguson, and M. Razeghi, *J. Vac. Sci. Technol. B* **13**, 782 (1995).
⁸K. J. Goldammer, W. K. Liu, G. A. Khodaparast, S. C. Lindstrom, M. B. Johnson, R. E. Doezema, and M. B. Santos, *J. Vac. Sci. Technol. B* **16**, 1367 (1998).
⁹W. K. Liu, K. J. Goldammer, and M. B. Santos, *J. Appl. Phys.* **84**, 205 (1998).
¹⁰N. Dai, F. Brown, P. Barsic, G. A. Khodaparast, R. E. Doezema, M. B. Johnson, S. J. Chung, K. J. Goldammer, and M. B. Santos, *Appl. Phys. Lett.* **73**, 1101 (1998).
¹¹B. Etienne and E. Paris, *J. Phys.* **48**, 2049 (1987).
¹²M. Shayegan, V. J. Goldman, M. Santos, T. Sajoto, L. Engel, and D. C. Tsui, *Appl. Phys. Lett.* **53**, 2080 (1988).
¹³The data shown in Fig. 2 is for wafer pieces with morphologies typical of the majority of the wafer area. The two additional lower-mobility samples in Fig. 5 are pieces from the edge of a wafer. For some wafers, the morphology at the edges is noticeably worse than at the center.